Moisture Movement Through Cracked Clay Soil Profiles

Geotechnical and Geological Engineering
An International Journal

ISSN 0960-3182
Volume 28
Number 6

Geotech Geol Eng (2010)
28:865-888
DOI 10.1007/s10706-010-9349-x

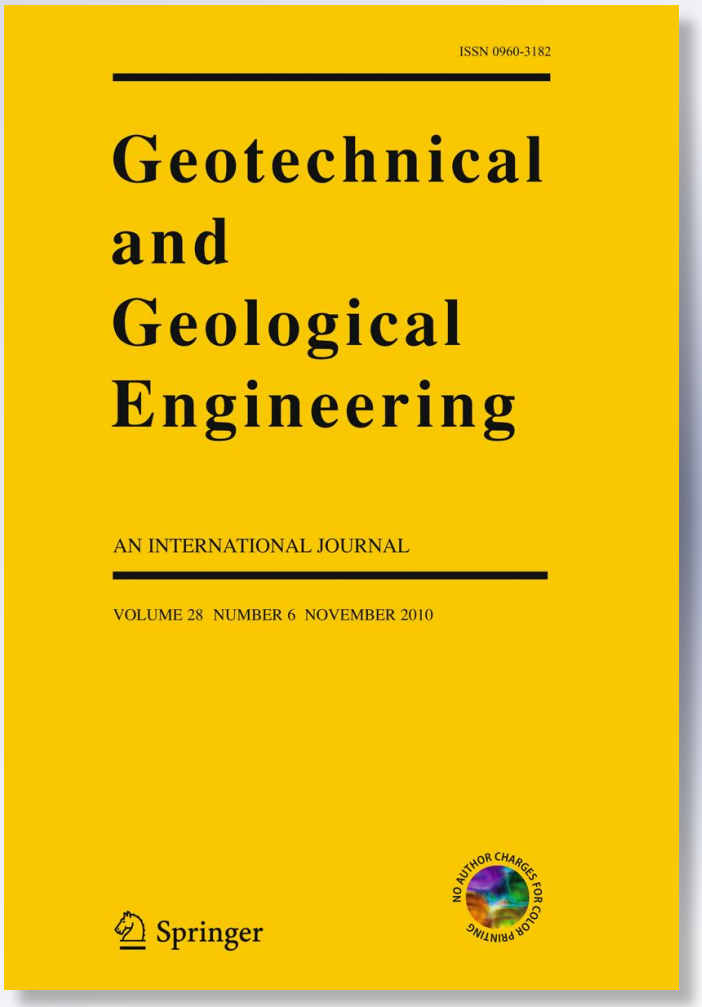

Springer

Geotech Geol Eng (2010) 28:865–888
DOI 10.1007/s10706-010-9349-x

ORIGINAL PAPER

Moisture Movement Through Cracked Clay Soil Profiles

Delwyn G. Fredlund · Sandra L. Houston · Quan Nguyen · Murray D. Fredlund

Received: 7 April 2009 / Accepted: 19 July 2010 / Published online: 29 July 2010

Abstract A continuum mechanics approach is used for the formulation of unsaturated hydraulic conductivity functions and the water storage functions for fractured or cracked clay soils in this parametric study. Suggested procedures are based on available research literature related to the behavior of cracked unsaturated porous media. The soil–water characteristic curve, hydraulic conductivity and water storage functions take on the character of bi-modal unsaturated soil property functions. The bimodal character arises out of the independent behavior of the cracks and the intact clay soil. Matric suction changes beneath a slab-on-grade foundation placed on a cracked clay soil profile are modeled for varied surface flux conditions using the proposed unsaturated hydraulic conductivity and water storage functions. The impact of various levels of surface cracking on soil suction distributions is discussed. Suction distribution patterns are dependent on the initial soil surface suction. In particular, the results are dependent upon whether the initial matric suction is less than or greater than the air entry of the cracked clay. There is an extremely wide range of possible conditions that could be modeled but the parametric study results presented in this paper are limited to a series of selected crack widths and densities for an exfiltration case and an infiltration case.

Keywords Unsaturated soils · Cracked clay · Unsaturated flow · Unsaturated soil properties

D. G. Fredlund
Golder Associates, Saskatoon, SK S7H 0T4, Canada

S. L. Houston (✉)
Arizona State University, Tempe, AZ, USA
e-mail: sandra.houston@asu.edu

Q. Nguyen
Golder Associates Pty Ltd, Brisbane, Australia

M. D. Fredlund
SoilVision Systems Ltd, Saskatoon, SK S7N 1A9, Canada

1 Introduction

Clay soils start to crack from the ground surface as matric suction increases. The low confining pressures near the ground surface allows clay soils to commence cracking at relatively low matric suctions. The cracks generally become closed with depth as the confining pressure increases. It is difficult to estimate the hydraulic conductivity and the water storage properties of the cracked clay (i.e., fissured and fractured clays).

The behavioral physical processes of hydraulic conductivity and the water storage associated with a cracked soil are notably different from those of an intact soil. Unsaturated soil mechanics developments have focused on independently understanding and describing changes in hydraulic conductivity and water storage as the matric suction in a soil is changed. Independent empirical, unsaturated soil property

functions have been proposed, formulated and tested for both hydraulic conductivity and water storage (Fredlund and Rahardjo 1993). Essentially all proposed empirical functions bear a relationship to the soil–water characteristic curve, SWCC, of the soil. The unsaturated soil property functions for hydraulic conductivity and water storage are generally used in an independent manner when solving the partial differential equation describing moisture flow through an unsaturated soil. While these empirical soil property functions have been proposed and studied for intact soils, little attention has been given to suitable unsaturated soil property functions for cracked soils.

The objectives of this paper are to: (1) formulate an empirical model for the hydraulic conductivity and water storage functions for a cracked, unsaturated soil, and (2) use the proposed unsaturated soil property functions for a parametric study to illustrate the effect that cracks have on moisture movement in and out of a cracked, unsaturated soil. The study is restricted to viewing changes in soil suction in response to the application of ground surface moisture flux (i.e., infiltration and evaporation). Conditions related to anisotropy and hysteresis of the cracked material and volume change in cracked soils (e.g., shrink/swell of expansive clays) constitute independent, separate studies which are currently under investigation by the authors. The assumption is made that volume changes associated with matric suction changes are small. This behavior is known to not rigorously describe "real world" cracked, clay soils. Similarly, crack patterns were simplified in these analyses to study the effect of varying width, spacing, depth, and volume of cracks. The crack patterns were not necessarily intended to be entirely consistent with patterns observed in the field. The parametric study presented provides a starting point for examining the behavior of cracked clays.

A review of the existing research literature on the behavior of cracked soils is summarized and some information is available on characterizing the hydraulic conductivity and the water storage functions for cracked clay soils. These functions have then been used to model infiltration and evaporation from the soil. Both the hydraulic conductivity and water storage functions take on the character of a bimodal unsaturated soil property function because of extremely different conditions introduced by cracks in the soil. An intact soil theoretically becomes less pervious as matric suction increases; however, at the same time cracks can occur that change the overall soil mass permeability considerably. This study focuses on the prediction of matric suction changes throughout the soil mass as various ground surface flux conditions are imposed.

The hydraulic conductivity and water storage functions for an unsaturated porous medium are necessary input parameters required when modeling water infiltration or exfiltration from a soil. It is time consuming, demanding and costly to experimentally measure the hydraulic conductivity and water storage functions for an unsaturated soil. The challenge becomes even greater when dealing with cracked porous medium. Estimations of these functions from a soil–water characteristic curve have become a less costly and a more attractive procedure for many geotechnical engineering problems. This study focused on the estimation of suitable unsaturated soil property functions for cracked clay soils, assuming that the cracked soil can be modeled as a continuum.

2 Review of Models for the Flow of Water in a Saturated Fractured Media

Fractures (cracks) in a soil mass dramatically change the mechanical and hydrological behavior of a porous medium. The fractures reduce shear strength and increase the saturated hydraulic conductivity of the soil. The fractures provide a preferential flow pathway and the hydraulic conductivity of the soil is significantly increased (Snow 1965; Novák et al. 2000; Liu et al. 2004). Keller et al. (1985) studied the hydraulic conductivity of a weathered till (i.e., fractured glacial till) and found that the saturated hydraulic conductivity was approximately two orders of magnitude higher than its intact matrix hydraulic conductivity.

Significant progress has been made since the 1960s in numerical modeling of flow and transport processes in fractured porous media. Research has been driven by an increasing need to develop petroleum and geothermal reservoirs, other underground resources, and to resolve subsurface contamination problems. Numerous numerical models have been developed using a variety of techniques (Barenblatt et al. 1960; Warren and Root 1963; Kazemi 1969; Pruess and Narasimhan 1985).

Prior to the 1990s, most studies only considered the flow of water through the fracture system in fractured rocks (i.e., matrix system was assumed to be impermeable). After the 1990s, many models have taken into account the flow of water through the matrix system as well as flow through the fractures and recent research has considered the interface fracture/matrix flow. Researchers have developed and applied a variety of different conceptual models and modeling approaches for the flow of water through saturated fractured porous media (Berkowitz 2002). Wu and Pruess (2005) categorized the models for fractured and cracked media into three categories; namely, (1) an explicit discrete-fracture and matrix model (e.g., Snow 1965; Stothoff and Or 2000), (2) a dual-continuum model, including double- and multi-porosity, dual-hydraulic conductivity, or a more general "Multiple Interacting Continua"'(MINC) model (e.g., Barenblatt et al. 1960; Warren and Root 1963; Kazemi 1969; Pruess and Narasimhan 1985), and (3) an effective-continuum model (e.g., Wu 2000).

Discrete fracture network models have been implemented for the study of groundwater flow in which fractured rock is assumed to consist of two components; namely, the fracture network and the porous rock matrix. The fracture network consists of large fractures that control groundwater flow through the rock mass. The porous rock matrix plays a secondary role in groundwater flow. The application of this model is currently limited because of the computational intensity involved, as well as an inability to obtain a detailed understanding of the fractures and the matrix geometric properties as well as the associated spatial distributions of fractures at a given site.

Dual-continuum approaches include the classic *double porosity* model (Barenblatt et al. 1960; Warren and Root 1963; Odeh 1965), the dual-hydraulic conductivity concept, and the more rigorous dual-continuum generalization (Pruess and Narasimhan 1985) for modeling flow through fractured porous mediums. In the double-porosity model, a flow domain is composed of matrix blocks with low hydraulic conductivity embedded in a network of interconnected fractures. This model treats matrix blocks as spatially distributed sink or source loadings to the fracture system. Because of the computational efficiency of this approach and its ability to simultaneously match many types of laboratory or field-observed data (e.g., Kazemi 1979; Wu et al. 1999), the dual-continuum model has perhaps been the most widely used method in petroleum and geothermal engineering, as well as in groundwater hydrogeology. The dual-continuum method is conceptually simpler and computationally much less demanding than the discrete-fracture approach. Additionally, the dual-continuum method is able to handle fracture matrix interaction more easily than the discrete-fracture model, although there remains a question regarding how best to handle fracture-matrix interactions under different conditions (e.g., involving multiple phase flow).

3 Seepage Partial Differential Equation for an Intact or Cracked Soil

The general partial differential equation describing moisture flow through an unsaturated soil can be written as follows.

$$\frac{\partial}{\partial x}\left(k_x\frac{\partial h}{\partial x}\right)+\frac{\partial}{\partial y}\left(k_y\frac{\partial h}{\partial y}\right)=\rho_w g m_2^w\frac{\partial h}{\partial t} \tag{1}$$

where: h = hydraulic head in the water phase; t = time; k_x, k_y = hydraulic conductivity in the x- and y-coordinate directions, respectively; ρ_w = density of water; g = gravitational acceleration and $m_2^w=\frac{\partial\theta_w}{\partial\psi}$ = coefficient of water volume change with respect to soil suction. The primary soil properties involved in this equation are the hydraulic conductivity function and the water storage function. The hydraulic conductivity and the water storage functions are both related to the soil–water characteristic curve of the material. The intact soil matrix forms one part of the overall model and the cracks in the soil form the other part of the soil–water characteristic curve for the "cracked clay".

3.1 SWCC Model for the Intact Soil

The soil–water characteristic curve data obtained from a laboratory test consists of a series of disconnected points. A mathematical equation is usually best-fit to the data to provide the SWCC functional relationship for modeling. Numerous curve-fitting equations for soil–water characteristic curves can be found in the literature (Gardner 1958; Brooks and

Corey 1964; van Genuchten 1980; Mualem 1976; Fredlund and Xing 1994). Thirteen different soil–water characteristic curve-fitting equations were evaluated by Leong and Rahardjo (1997) and it was found that all three-parameter equations (i.e., a, n, and m) perform somewhat better than two-parameter equations (i.e., a, and n) for best-fitting experimental data.

3.2 Generation of the SWCC Model for a Cracked Material

Zhang and Fredlund (2004) suggested the use of rock mechanics theory for defining the soil–water characteristic curve of a material containing cracks. The soil was assumed to be non-swelling. The SWCC was based on the pore size distribution curve for the material. The pore size distributions for both the matrix and the fracture network were assumed to follow a modified lognormal distribution. Zhang and Fredlund (2004) explained that a fractured rock will produce a bimodal material with a matrix phase and a fracture phase. The overall soil–water characteristic curve will be the sum of the effects of the two material phases weighted according to the respective porosities. The authors also assumed that the combined matrix and fracture medium qualified as a continuum with the same suction value applying for the two overlapping porous continua. A computed soil–water characteristic curve for the rock matrix, the fractures and the entire fractured rock mass is shown in Fig. 1. The assumption that the cracked media behaves as a continuum is further explored in the analyses of cracked clay presented in this paper. The soil was assumed to be non-swelling, and interactions between the cracks and the intact soil are not directly considered. It was assumed that the cracks and the intact clay combine to form a continuum with a continuous function that contains saturated–unsaturated soil parameters.

Figure 1 shows that the soil–water characteristic curve for the rock matrix approaches the SWCC for the entire rock mass once the residual suction in the fractures are exceeded. At high degrees of saturation the role of the fracture network dominates behavior. The soil–water characteristic curve for a cracked soil may also be assumed to take on a bi-modal character. Existing bimodal models for SWCC relationships from the geotechnical and soil science literature can be applied to a cracked medium. Several mathematical models that have a bimodal character for the SWCC are available (Durner 1994; Burger and Shackelford 2001; and Gitirana and Fredlund 2004).

3.3 Review of Water Storage Function for a Soil

The coefficient of water storage indicates the amount of water taken on or released from the soil in response to a change in soil suction. The water storage function can be defined as the (arithmetic) slope of the soil–water characteristic curve and can be calculated directly from the SWCC of the soil. Figure 2 shows a plot of a water storage function developed from a bimodal SWCC. The water storage function becomes highly nonlinear as the soil desaturates. Sillers et al. (2002) presented a series of

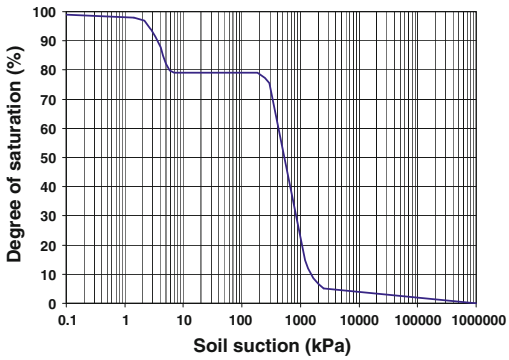

Fig. 1 Relationship between degree of saturation and soil suction (Zhang and Fredlund 2003)

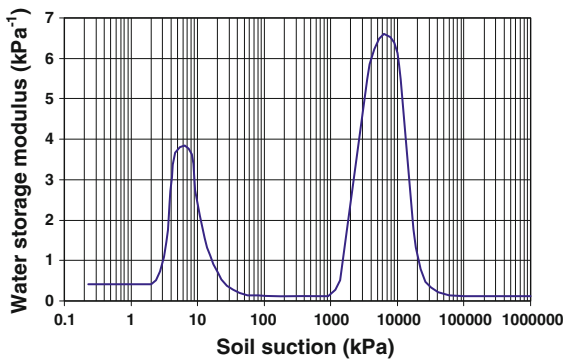

Fig. 2 A typical coefficient of water storage for a bi-modal material

coefficient of water storage functions by differentiating various SWCC equations.

4 Review of Unsaturated Hydraulic Conductivity Functions for Intact Materials

Numerous empirical models have been proposed to predict the hydraulic conductivity function of an unsaturated soil. These models use the soil–water characteristic curve and the saturated hydraulic conductivity to compute the unsaturated hydraulic conductivity function. For intact soils, several statistical hydraulic conductivity models based on soil–water characteristic curves are available (Burdine 1953; Brooks and Corey 1964; Mualem 1980; Brooks and Corey 1964; Mualem 1976; van Genuchten 1980; Fredlund and Xing 1994; Kunze et al. 1968; Mualem 1976; Assouline 2001).

5 Review of Hydraulic Conductivity Models for Unsaturated Fractured Media

The measurement of the hydraulic conductivity for an unsaturated, cracked soil is extremely difficult. Consequently, estimation procedures become extremely attractive for the unsaturated soil property functions for a cracked soil. It appears reasonable to use methods that superimpose the SWCC for the intact portion of the soil with another independent analysis for the fractured portion. The resulting SWCC has also been used to estimate the hydraulic conductivity of a cracked medium (Peters and Klavetter 1988; Mallant et al. 1997; Köhne et al. 2002; Liu et al. 2004; Zhang and Fredlund 2004).

One of the first challenges associated with predicting the hydraulic conductivity of a cracked soil is determining the SWCC for the fractured portion. There will be a drying (desorption) curve and a wetting (adsorption) curve for each soil. Only a single curve (e.g., the desorption curve) is given consideration in this study, and thus, hysteresis in the cracked soil is neglected as a first approximation. Once the SWCC is established for the cracked soil, independent estimation procedures must then be used to compute an appropriate hydraulic conductivity function for the intact and cracked portions. Most permeability models developed to-date are for intact porous media and are based on a continuum mechanics approach. The use of these models for the cracked fracture network is questionable because the geometry of a fractured network is quite different from the pore geometry of an intact soil.

Peters and Klavetter (1988) proposed a continuum mechanics model for the flow of water through an unsaturated fractured rock mass. It was assumed that the fracture conductivity for water movement across the fracture (i.e., through contact points) was considerably larger than flow through the adjacent matrix. In flow calculation, the fracture conductivity for water movement across the fractures was replaced by the matrix conductivity. The average fracture conductivity for water movement in the plane of the fracture proved to be a highly nonlinear function of fracture saturation and the suction in the matrix material. Both macroscopic and microscopic approaches were used to develop the model. The macroscopic model assumes that the fractures and matrix hydrologic parameters are statistically representative of a large volume of the rock mass. A fluid flow equation is written for both the matrix and the cracked medium. The microscopic approach uses a representation of the actual physical structure of the system combined with fundamental theoretical considerations given to fluid flow through pores with a specific geometry. Peters and Klavetter (1988) used the Burdine (1953) and the Mualem (1976) models for the prediction of the hydraulic conductivity function. The authors found that the calculated permeability functions using both approaches yielded similar results.

Mallant et al. (1997) and Köhne et al. (2002) evaluated the use of multimodal hydraulic conductivity functions for characterizing a heterogeneous soil. The van Genuchten (1980) unimodal and multimodal soil–water characteristic curve equations along with the Mualem (1976) model were used for calculating the hydraulic conductivity of a structured unsaturated soil. It was found that the multimodal soil–water characteristic curve performed better than the unimodal soil–water characteristic curves. Chertkov and Ravina (2000) studied the shrinking-swelling phenomenon of clay soils through use of a capillary-crack network. The soil–water characteristic curve for the cracked soil was determined by using the total crack volume and the volume of water-filled cracks. A generalization of the van Genuchten (1980),

Mualem (1976) model was used for the hydraulic conductivity function. A comparison between the measured data and the predicted hydraulic conductivity showed good agreement.

Liu and Bodvarsson (2001) studied the use of the van Genuchten (1980) and Brooks and Corey (1964) models for the hydraulic conductivity of a fracture rock and found that the methods generally underestimated the hydraulic conductivity values. The authors proposed a new model for the hydraulic conductivity of a fractured porous media by modifying the Brooks and Corey (1968) model.

6 Current Study of Unsaturated Flow Through Cracked Clay

Two basic saturated–unsaturated soil property functions must be known when attempting to quantify water flow through a cracked clay. These functions are: (1) the relationship between soil suction and the water content of the soil; and (2) the relationship between soil suction and the hydraulic conductivity.

Crack width and crack spacing in 2 or 3 dimensions provide the basic information required to construct a theoretical equation for the relationship between water content and soil suction in a cracked soil. A simple conceptualization of the actual distributions of cracks in a fractured soil is used in this study. Film flow and vapor transport are ignored and the focus is on flow associated with cracks in an unsaturated cracked soil which is assumed to act as a continuum with bimodal property functions.

6.1 SWCC Generation for a Bi-Modal Soil

A clay soil was assumed as the basic soil for this study. There are two parts to the SWCC model; namely, an intact portion and another portion that represents the cracked portion. The soil–water characteristic curve data for the intact portion of the soil is typical of what might be measured for clay. The saturated hydraulic conductivity, k_s, of the intact portion was assumed to be 10^{-7} (m/s). The cracked clay is assumed to exhibit bimodal behavior. The SWCC for the bimodal soil can be generated once the soil–water characteristic curve for the fractured portion is determined.

7 Generation of the SWCC for a Cracked Soil

The model selected for unsaturated flow though a cracked, porous medium is based on capillary theory (e.g., Peters and Klavetter 1988). A relationship is assumed between pore size (i.e., crack width) and matric suction. The degree of saturation of the cracked soil becomes related to soil suction. The crack width and crack spacing are analyzed by assuming fixed values. The primary steps in implementing this conceptual model are shown in Fig. 3. The crack widths and spacings are varied over a wide range of values to evaluate the effect on computed soil suction. While there was no specific intent to duplicate field crack conditions in this study, the larger crack widths evaluated (e.g. 1 mm) are likely representative of some in situ conditions.

First, the width of the cracks and the spacing between cracks are assumed for one cubic meter of soil. In this study the width of cracks was assumed to be 0.05 mm, 0.1 mm, 0.5 mm, 1 mm and the spacing between cracks was taken as 10 cm, 5 cm, 1 cm and 0.5 cm. The percentage of the total volume that is open fractures was then calculated. The specific gravity of the clay, $G_S = 2.83$, the gravimetric water content, w is equal to 35% when the degree of saturation, S, is 100%.

The soil–water characteristic curve for the entire cracked soil can be established through use of a bimodal fitting equation. These fitting equations will define two distinct air-entry values and two residual points on the bimodal SWCCs. The curve-fitting parameters also define the slopes between the bending points along the SWCC. Once data points for the entire cracked soil are obtained, the results can be input into the SoilVision (Fredlund 1996) software for the computation of the best-fit mathematical equation.

The Fredlund and Xing (1994) SWCC equation and the Fredlund Bimodal (1999) SWCC equation were used in this study. The Modified Campbell pseudo-transfer function, PTF (Fredlund 1996) was based on the Fredlund Bimodal equation and a correction factor was applied in the high soil suction range to yield a suction of 1,000,000 kPa at zero water content (Eq. 2). The same equation without the correction factor applied at high soil suction (Leong and Rahardjo 1997) (Eq. 3) was also used to generate the SWCCs in this study.

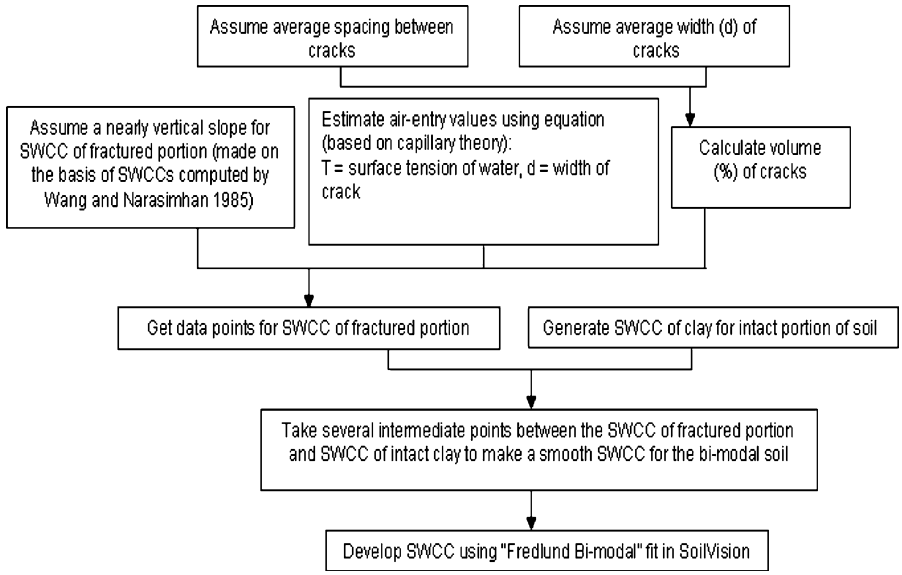

Fig. 3 Flowchart for the generation of the bi-modal SWCCs

$$w(\psi) = w_S \left\{ V \left[\frac{1}{\ln\left(\exp(1) + \left(\frac{a_f}{\psi}\right)^{n_f}\right)^{m_f}} \right] + (1-V) \left[\frac{1}{\ln\left(\exp(1) + \left(\frac{j_f}{\psi}\right)^{k_f}\right)^{l_f}} \right] \right\} \left[1 - \left(\frac{\ln\left(1 + \frac{\psi}{3000}\right)}{\ln\left(1 + \frac{1000000}{3000}\right)} \right) \right] \quad (2)$$

$$w(\psi) = w_S \left\{ V \left[\frac{1}{\ln\left(\exp(1) + \left(\frac{a_f}{\psi}\right)^{n_f}\right)^{m_f}} \right] + (1-V) \left[\frac{1}{\ln\left(\exp(1) + \left(\frac{j_f}{\psi}\right)^{k_f}\right)^{l_f}} \right] \right\} \quad (3)$$

where: w_s = water content (either volumetric or gravimetric) at saturated conditions; a_f and j_f = curve-fitting parameters related to the air-entry values of the intact and fractured portions, respectively; n_f and k_f = curve-fitting parameters related to the slopes of the intact and fractured portions, respectively; m_f and l_f = curve-fitting parameters related to the residual water contents of the intact and fractured portions, respectively; and V = normalized volume of the intact portion to the total volume.

The term $\left[1 - \left(\frac{\ln\left(1+\frac{\psi}{3000}\right)}{\ln\left(1+\frac{1000000}{3000}\right)} \right)\right]$ in Eq. 2 forces the generated curves to pass through a soil suction of 10^6 kPa at zero water content.

The bimodal SWCC equations (i.e., Eqs. 2 and 3) are linearly weighted with respect to the matrix volume and the crack volumes (or water contents). The soil–water characteristic curves are an extended form of the unimodal equations proposed by Fredlund and Xing (1994). Data points on the soil–water characteristic curve corresponding to the cracked portion are generated first. Using the SWCC for the intact soil, it is possible to derive the SWCC for the entire cracked soil mass.

Four sets of crack widths and four crack spacings were assumed. Therefore, 16 sets of different cracked soil conditions were obtained, and 3 different depths of these cracks were analyzed. A sample SWCC for the cracked clay is shown in Fig. 4 for a crack width of 1 mm and a crack spacing of 0.5 cm. Figure 4 shows the distinct gap between the section representative of the cracked portion and the section

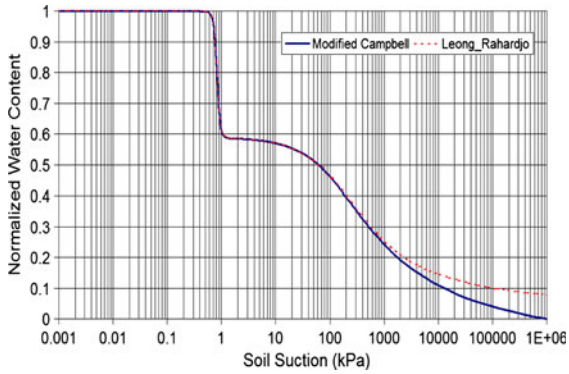

Fig. 4 Soil-water characteristics curve for fractured clay (1 mm @ 0.5 cm)

representative of the intact portion. Two methods were used in generating the SWCCs; namely, the Leong and Rahardjo (1997) method and the Modified Campbell (Campbell 1973) method. The air-entry value for the crack-dominated sections reduces as the crack width is increased. Also, the gap between the two bend points in the SWCC becomes greater as the crack width is increased.

8 Hydraulic Conductivity Function for the Cracked Expansive Soil

To evaluate the hydraulic conductivity function for the cracked soil, it is necessary to first determine the saturated hydraulic conductivity for the cracked soil mass. The steps for obtaining the hydraulic conductivity of the cracked unsaturated clay are described in the flowchart shown in Fig. 5. The hydraulic conductivity function for a cracked soil cannot be obtained by simply integrating along the bimodal SWCC. Rather, it is necessary to treat the cracked soil portion and the intact soil portion independently.

A super-position procedure was used where the cracked portion and the intact portion are treated as two independent materials. Each must be started from

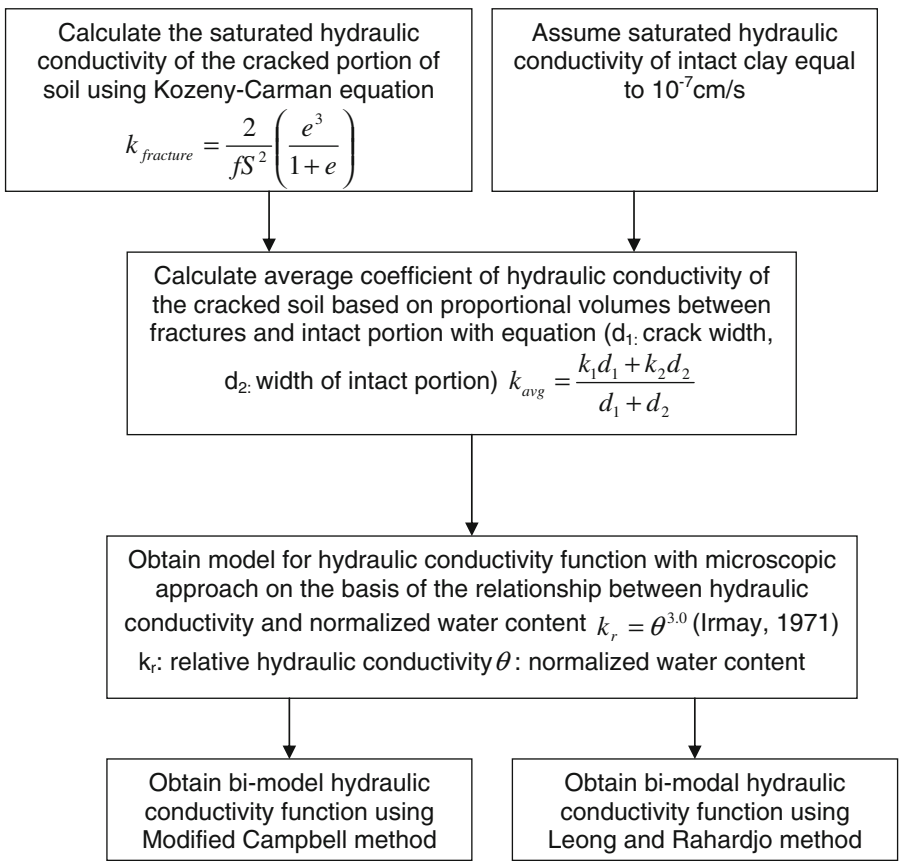

Fig. 5 Procedure for obtaining the hydraulic conductivity function for a fractured soil

the correct saturated conditions. Then the two independent hydraulic conductivity functions need to be combined to give the unsaturated soil property function for the composite material.

9 Determination of Saturated Hydraulic Conductivity for the Cracked Portion

Kozeny (1927) proposed an equation to relate particle size, porosity (n), angularity of particles, specific surface area (A) and viscosity of water (η_w) to hydraulic conductivity. Carman (1939) modified this equation and replaced porosity, n, with void ratio, e, using the relationship, $n = \frac{e}{1+e}$. The equation is known as the Kozeny-Carman equation:

$$k = \frac{\rho_w g}{C\eta_w A^2}\frac{e^3}{1+e} \tag{4}$$

For a collection of spherical particles that are uniformly distributed in size between diameters d_1 and d_2, the specific surface area, A, can be computed from the equation,

$$A = \frac{6}{\sqrt{(d_1 d_2)}} \tag{5}$$

If d_1 and d_2 are expressed in millimeters, A is expressed as mm^2/mm^3, or mm^{-1}. The term $\sqrt{d_1 d_2}$is known as the geometric mean particle diameter. The constant, C is a shape factor that is equal to 5 for spherical particles. Equation 5 was developed for water flow between particles but has modified for flow through cylindrical pipes, between plates and other geometries (Wu 1976). An angularity factor, f, has been used as part of the formulation for this study to account for flow through cracked soils. The authors are uncertain regarding the most appropriate angularity factor, f, that should be used but have simply adopted a value of 1.1 for the present study. Hopefully, further research will reveal the most suitable angularity factor to use for infiltration modelling purposes. However, the numerical results are not highly sensitive to the f value. Equation 4 can be expressed in SI units and the variables are defined as follows: k = hydraulic conductivity, m/s, g = acceleration due to gravity = 9.81 m/s^2, ρ_w = mass density of water = 1 Mg/m^2, η_w = dynamic viscosity of water at 20°C = 1 mPa, e = void ratio, and A = specific surface area of grains (mm^2/mm^3 or mm^{-1}).

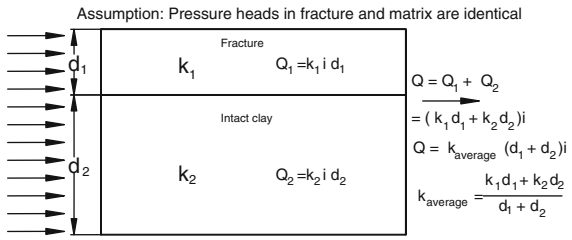

Fig. 6 Horizontal flow through the fractured soil

Substituting these values into Eq. 4 gives the following equation for hydraulic conductivity at 20°C,

$$k_{20} = \frac{(1000)(9.81)}{5f\frac{1}{1000}(A*1000)^2}\frac{e^3}{1+e}(\mathrm{m/s}) = \frac{1.962}{fA^2}\frac{e^3}{1+e}(\mathrm{m/s}) \tag{6}$$

The following equation can be used for estimating the saturated hydraulic conductivity of the cracks or fractures.

$$k = \frac{2}{fA^2}\frac{e^3}{1+e}(\mathrm{m/s}) \tag{7}$$

10 Saturated Hydraulic Conductivity for the Entire Soil Mass

The average hydraulic conductivity for the entire cracked soil mass must be computed after the saturated hydraulic conductivity for the cracked portion has been computed. The cracked soil takes on the nature of an anisotropic soil. The average hydraulic conductivity for horizontal flow through a stratified soil can be calculated using Eq. 8. The rationale for using Eq. 8 is illustrated in Fig. 6:

$$k_{avg} = \frac{k_1 d_1 + k_2 d_2}{d_1 + d_2} \tag{8}$$

where: d_1 and d_2 are the depths of soil; k_1 and k_2 are the hydraulic conductivities of the respective soil layers.

11 Determination of the Unsaturated Hydraulic Conductivity Function for the Entire Soil Mass

The soil–water characteristic curve and the saturated hydraulic conductivity, k_{sat} of the entire cracked soil mass must be known before the unsaturated hydraulic conductivity function can be computed. The

following hydraulic conductivity function equation was used to compute the relative permeability (Irmay 1954, 1971).

$$k_r = \Theta^{3.0} \tag{9}$$

where k_r is the relative hydraulic conductivity, and Θ is normalized water content for the soil–water characteristic curve. The variable Θ is equal to the volumetric water content, θ_w, divided by the volumetric water content at saturation, θ_s. The hydraulic conductivity hereby becomes related to soil suction. The permeability functions were computed using the *SoilVision* software (Fredlund 1996). Other permeability versus soil suction functions could have been used but the primary purpose of this study is to illustrate the general role that cracks play in flow near the ground surface.

The hydraulic conductivity functions for various crack widths and crack spacing were computed for the cracked clay and an example function is presented in Fig. 7. This figure shows a distinct jump in the permeability functions between the facture-dominated material and the intact-dominated material. The computed hydraulic conductivity functions for the selected soil crack scenarios studied show that there is an increase of approximately one order of magnitude in hydraulic conductivity when the relative volume of cracks enlarges from 9% to 30%. Also, when comparing the bimodal SWCCs across this same volume of cracks (i.e., 9% to 30%), the difference in the bimodal hydraulic conductivity curves appear to be quite small. The hydraulic conductivities are weighted according to the relative volumes in the bulk material and therefore, the effect on the hydraulic conductivity curves can be relatively small. The air-entry value of the crack-dominated soil reduces from 7 kPa to 0.7 kPa when the crack widths increase from 0.05 mm to 1 mm.

12 Example Calculation of Soil Suctions in Cracked Clay Beneath a Slab

Numerical studies of seepage were performed using the bimodal functions for the cracked clay. Two initial suction conditions were considered in the analyses. The initial suction conditions were selected to show that flow in the cracked soil depends on soil suction conditions. If the initial suctions are higher than the air-entry value of the cracked domain, then insignificant flow will occur in the cracks. Otherwise, flow though the cracks can dominate the total amount of flow in the cracked clay at the beginning of infiltration.

The selected example problem involves an impermeable, flexible slab that is 12 m in width. The depth of the soil layer being modeled is 3 m. Because of symmetry, only half of the slab (i.e., 12 m from centerline) and soil were analyzed. The boundary conditions for the example problem are shown in Fig. 8. Two different surface flux conditions were selected; one corresponding to evaporation and the other to infiltration. The geometry for the cracks was varied and the analyses were performed for 3 different depths of cracks; namely, 0 m, 1 m and 2 m.

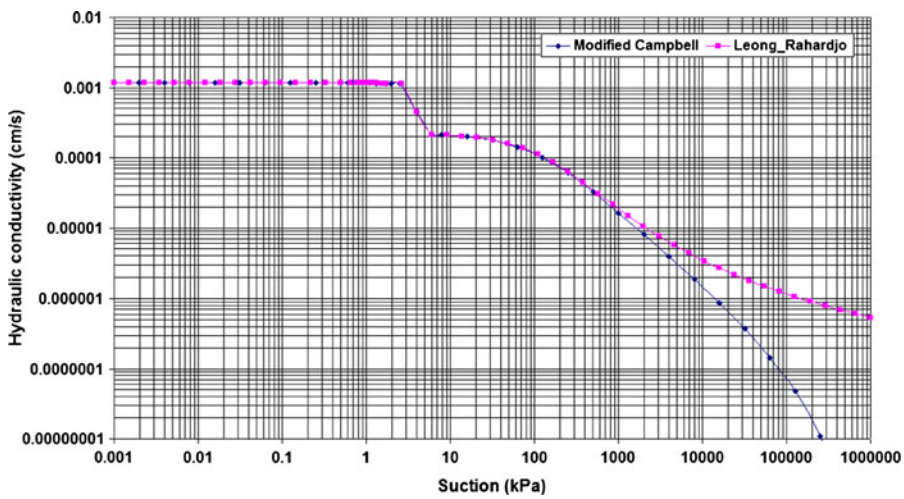

Fig. 7 Soil suction versus hydraulic conductivity for a fractured soil (crack of 0.1 mm wide at 0.5 cm spacing between cracks)

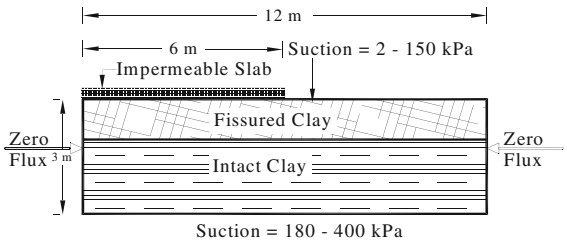

Fig. 8 Simulation of a fissured soil under an impermeable slab showing boundary conditions

13 Simulation of the Evaporation Case

The initial boundary conditions for the evaporation studies correspond to steady state conditions established using *SVFlux*. The evaporation rate for a transient analysis was then imposed at 4 mm/day over the exposed ground surface. Transient seepage analyses were performed for the following conditions; namely, no cracks in the soil, 1 m and 2 m depths of cracks.

14 Intact Soil: No Cracks

The changes in matric suction along the surface of the soil, and vertical profiles of suction at the edge and center of the flexible slab are shown for the case when the soil is not cracked. The analysis was performed for 7 days of evaporation and the results are shown here for the initial conditions and elapsed times of 1 day, 3 days, 5 days and 7 days (Figs. 9, 10, 11).

Figure 10 shows that the matric suctions along the ground surface increased significantly in the region outside the slab as a result of evaporation. The suctions changed from 2 to 200 kPa when there was an evaporation rate of 4 mm/day applied for 7 days. The suctions under the impermeable slab remained relatively constant for this same 7 day period of evaporation. The difference in suction between the slab center and the slab edge is clearly shown in Figs. 10 and 11 which show vertical profiles of matric suction at the slab center and edge. The depth of impact of evaporation was greater at the slab edge (1 m) compared to the depth of influence at the slab center (0.5 m). The patterns of suction observed for the intact soil for a profile beneath the edge of the slab are shown in Fig. 11. The initial suction profile increases linearly with depth having a low suction at the ground surface and a suction of 180 kPa at the base boundary. As evaporation proceeds, there is an increase in suction at the soil surface and there is a curved pattern of suction change to a depth where matric suction (and hydraulic conductivity) is not affected by drying. The curvature of the suction profile at the base boundary is a boundary condition effect.

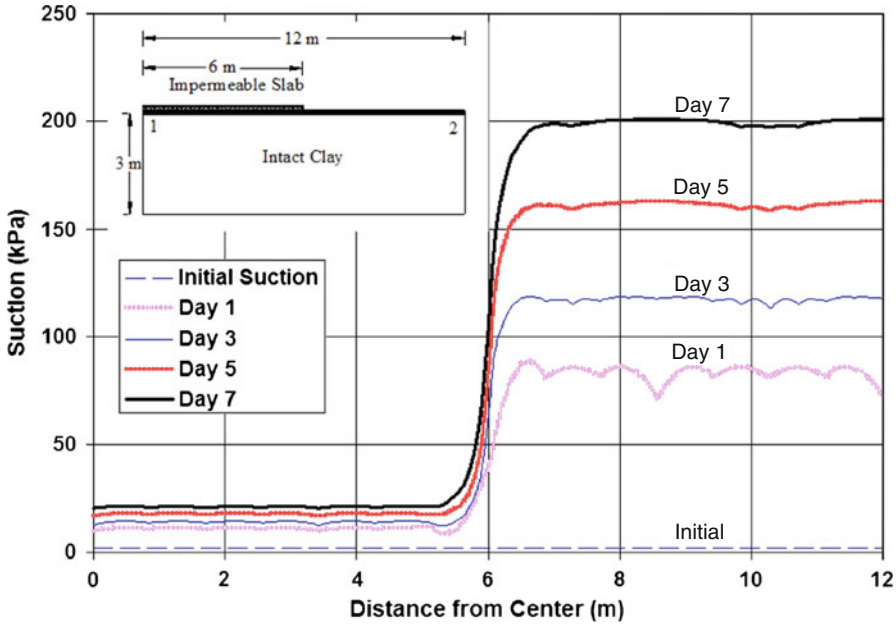

Fig. 9 Changes in matric suction along the ground surface (from point 1 to 2) for the intact clay during evaporation. Low initial suction

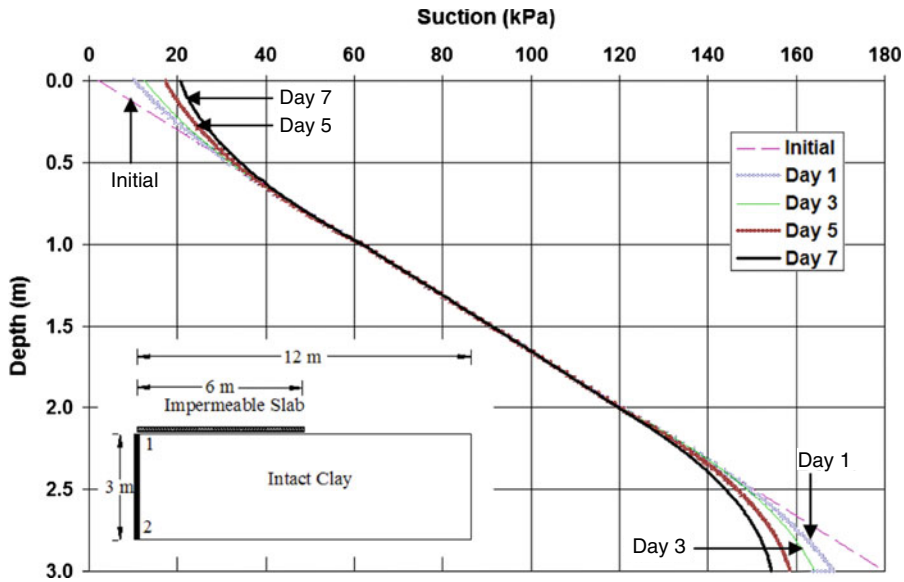

Fig. 10 Changes in matric suction beneath the center of the slab (from point 1 to 2) for intact clay during evaporation. Low initial suction

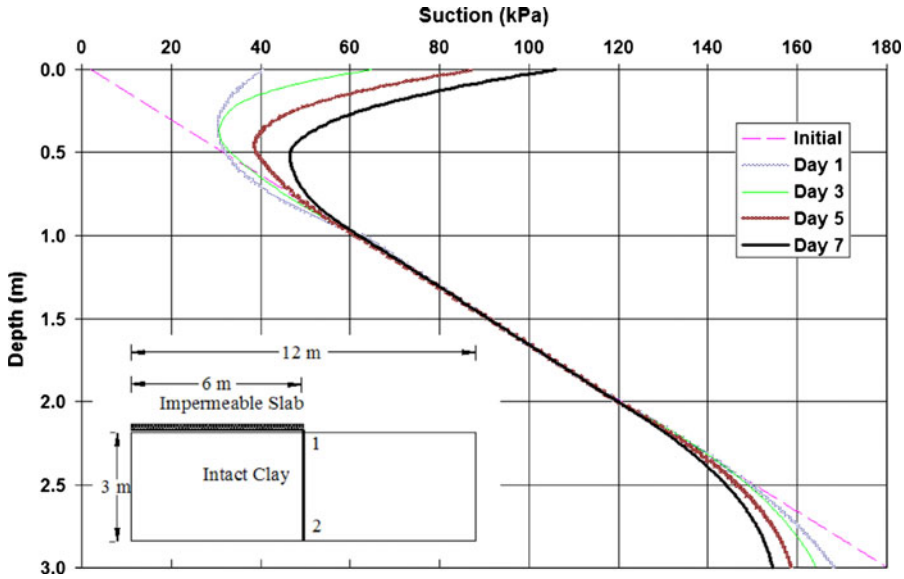

Fig. 11 Suction changes beneath the edge of the slab during evaporation from the intact clay. Low initial suction

15 Cracked Surface Soil With Initial Suction at Ground Surface Less Than Air-Entry Value

Simulations were performed with the initial suction at the ground surface less than air-entry value of the cracked soil. To illustrate suction changes with increasing width and reducing spacing of cracks, four conditions with varying crack width and spacing were considered, and two different crack depths were evaluated. Sample simulation results for a cracked soil depth of 1 m are shown in Figs. 12–17.

Matric suctions along the ground surface increase under evaporation conditions of 4 mm/day. When the crack width was increased and the crack spacing was decreased, the difference in matric suction between the soils covered by the slab and soils outside the slab reduced substantially as can be seen by comparing Figs. 12, 14, and 16. Horizontal flow dominated in the highly cracked soil region resulting in essentially the same ground surface soil suction conditions outside of the slab and beneath the slab (e.g. Fig. 16). Profiles of matric suction

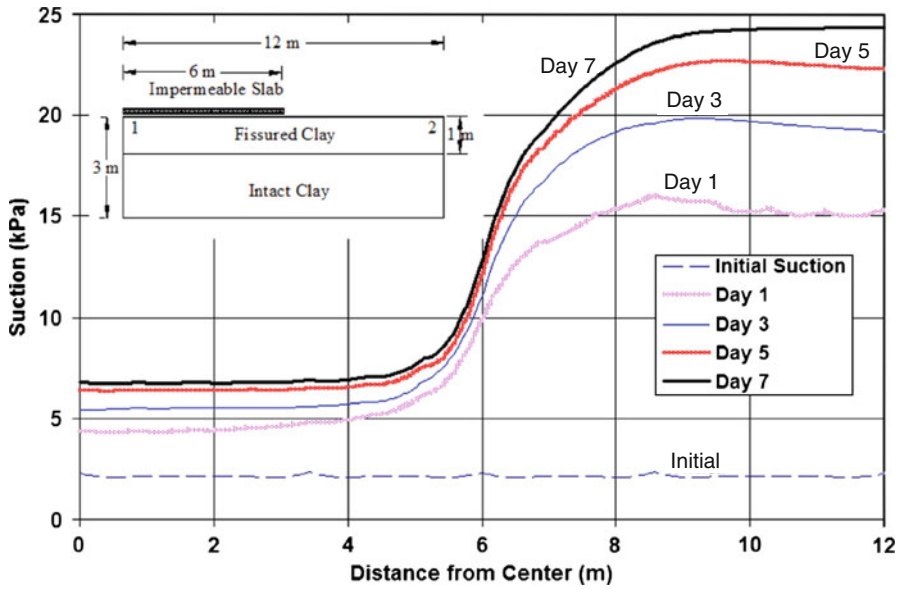

Fig. 12 Changes in matric suction along the surface (from point 1 to 2) for evaporation. Crack width of 0.05 mm at a spacing of 10 cm, initial suction less than the Air Entry Value of the cracked soil

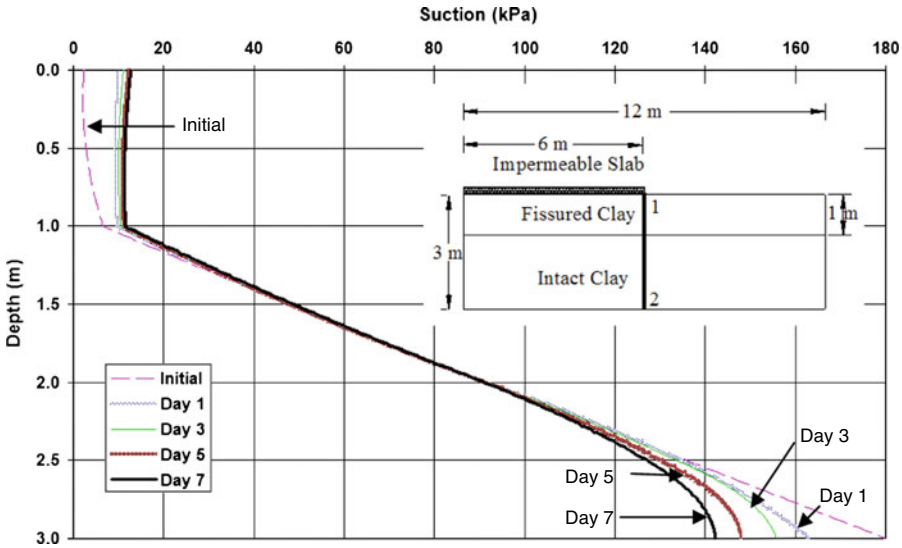

Fig. 13 Changes in matric suction beneath the edge of the slab (from point 1 to 2) for evaporation. Crack width of 0.05 mm at a spacing of 10 cm, initial suction less than the Air Entry Value of the cracked soil

versus depth at the center of the slab show that suctions increased significantly near the surface of the intact clay. The suction values in the cracked soil were essentially uniform (i.e., vertical profile of suction throughout the cracked clay), but varied nonlinearly in the intact clay. This pattern reflects the substantial difference in hydraulic conductivity between the intact and cracked soils (Fig. 15). The high hydraulic conductivity and low gradient within the cracked soil resulted in essentially vertical (constant with depth) profiles of suction within the cracked regions, for both low and high crack volumes (e.g., Figs. 13, 15, 17). It was observed that soil suction change was concentrated in the cracked soil region, with only minor soil suction changes in the intact clay beneath the cracked soil. Suction changes in the intact clay do not extend to significant depth even for the case where there is a high crack volume (Fig. 17). There were only small changes in matric suction for the intact soil at depth from 1.5 to 2.5 m for the 7 day evaporation time period considered.

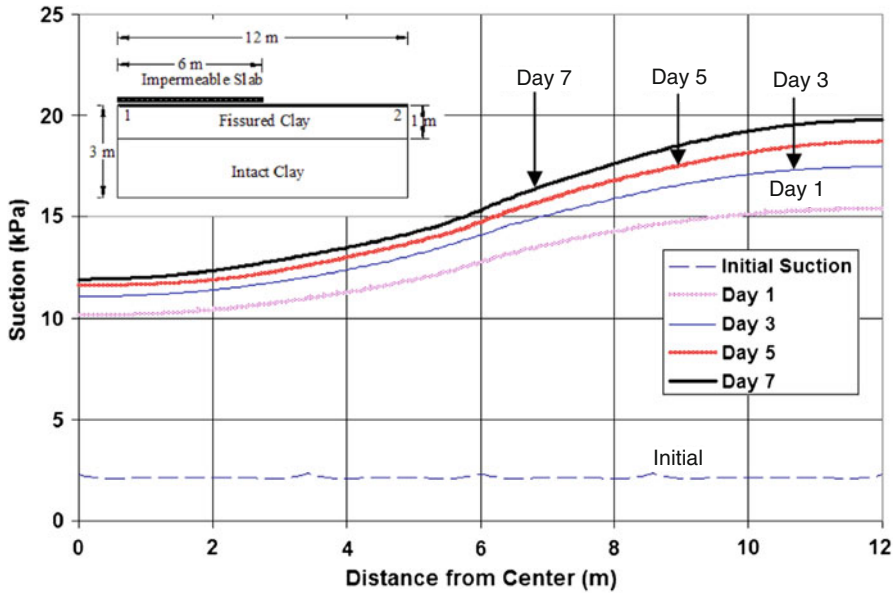

Fig. 14 Changes in matric suction along the ground surface (from point 1 to 2) for evaporation. Crack width of 0.05 mm at a spacing of 0.5 cm, initial suction less than the Air Entry Value of the cracked soil

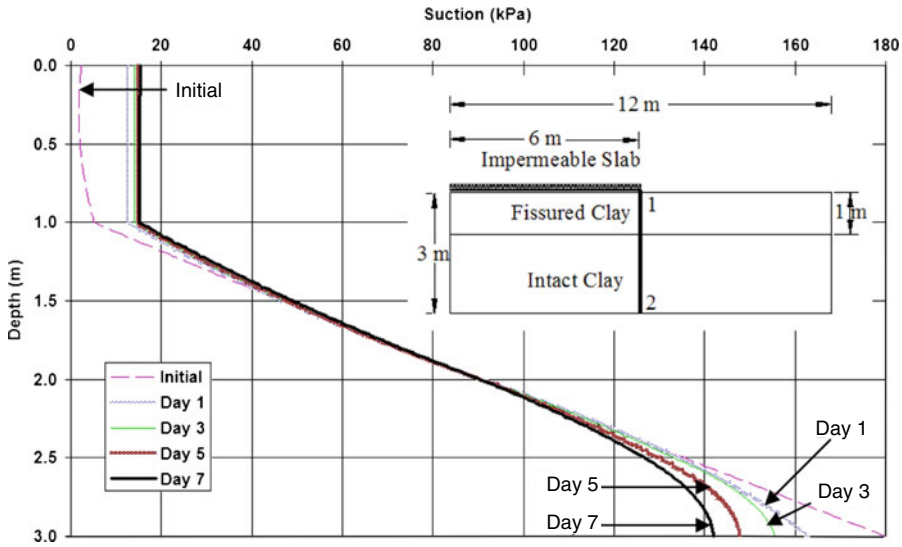

Fig. 15 Changes in matric suction along the depth at the slab beneath the edge of the slab (from point 1 to 2) for evaporation. Crack width of 0.05 mm at a spacing of 0.5 cm, initial suction less than the Air Entry Value of the cracked soil

Matric suctions generally increased significantly in the cracked soil during the first day of evaporation. The rate of change of suction decreased as the soil dried and the hydraulic conductivity decreased. For crack widths of 0.05 mm and crack spacings of 10 cm (low fracture volume), ground surface suction values increased from 2 kPa initial to 22 kPa after 7 days. For crack widths of 1 mm and a spacing of 10 cm (high crack volume) the ground surface matric suction increased to 53 kPa after 7 days of evaporation. The effect of the cracked soil surface was more pronounced for increasing crack widths compared to reducing crack spacing in that suction changes due to increasing the crack widths from 0.05 mm to 1 mm were higher than the suction change caused by reducing the spacing from 10 cm to 0.5 cm.

Although not presented in this paper, a crack depth of 2 m was considered for a number of evaporation cases. The higher crack depth resulted in a greater suction decrease at the ground surface compared to that observed for the 1 m crack depth. However, patterns of suction change were similar to those presented herein for the 1 m crack depth.

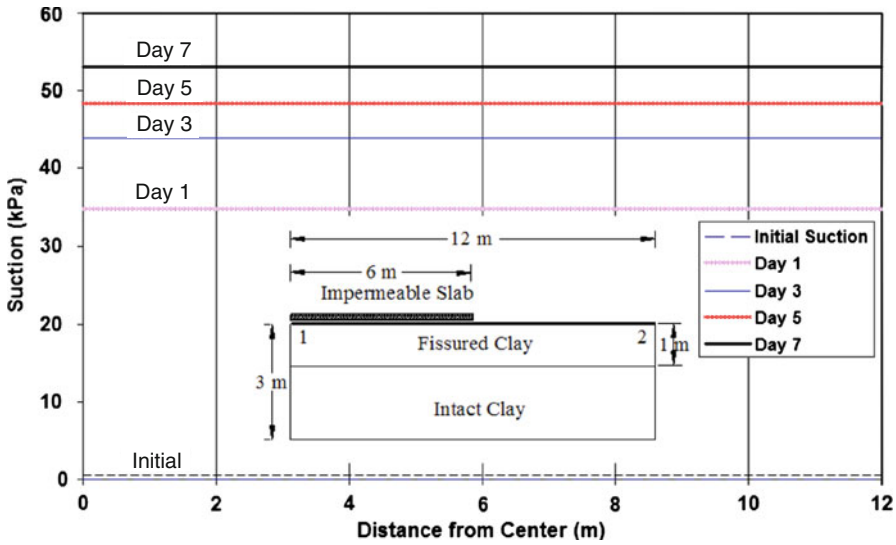

Fig. 16 Changes in matric suction along the ground surface (from point 1 to 2) for evaporation. Crack width of 1 mm at a spacing of 10 cm, initial suction less than the Air Entry Value of the cracked soil

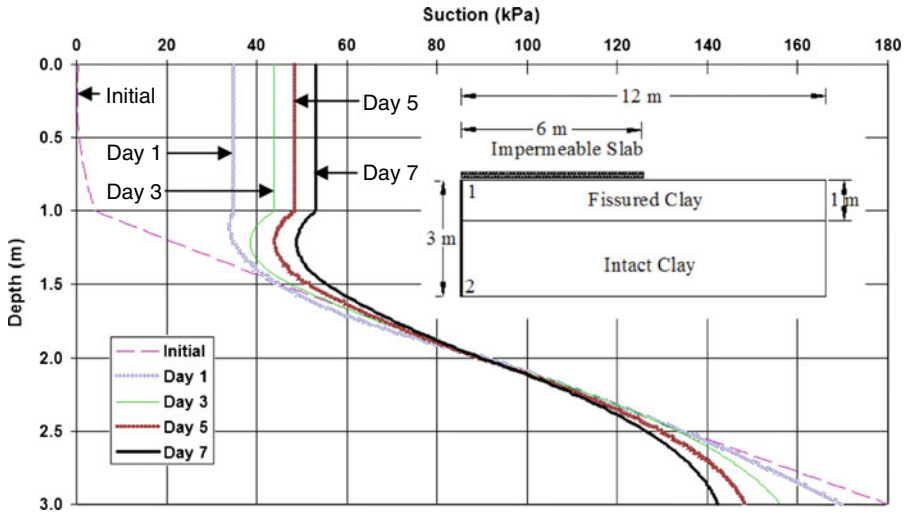

Fig. 17 Changes in matric suction beneath the center of the slab (from point 1 to 2) for evaporation. Crack width of 1 mm at a spacing of 10 cm, initial suction less than the Air Entry Value of the cracked soil

16 Cracked Soils With Initial Suction at Ground Surface Greater Than the Air-Entry Value

Simulations were also conducted with the initial suction at ground surface greater than the air-entry value of cracked soil. Again, four conditions of varying crack size and width were evaluated and two depths of cracked soil were considered. Sample simulation results for 1 m crack depth are shown in Figs. 18–24.

When there are cracks in the near-surface soil and the initial ground surface suctions are greater than the air-entry value of the cracked soil, the suction is higher outside the slab compared to beneath the slab for low to moderate crack volumes. This pattern is observed in the cracked clay region as well as in the intact clay (e.g., Figs. 18–20). For the cases of higher initial soil suction at the ground surface, the "action" with regard to suction change is in both the cracked soil and the intact clay. This occurs because there are small differences in the hydraulic conductivity of the cracked and intact soil. As a result, flow occurs primarily through the intact clay matrix rather than through the fractures.

When the crack width is increased, resulting in a larger crack volume, the hydraulic conductivity of the cracked soil increases significantly and horizontal moisture flow becomes dominant in the cracked soil. Therefore, evaporation causes near-surface soil suctions to increases both outside and beneath the slab

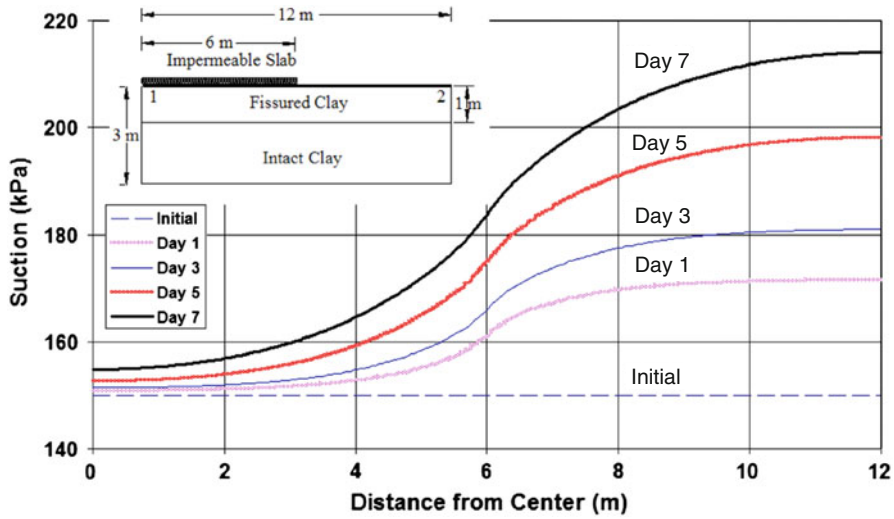

Fig. 18 Changes in matric suction along the ground surface (from point 1 to 2) for evaporation. Crack width of 0.05 mm at a spacing of 10 cm, initial suction greater than the Air Entry Value of the cracked soil

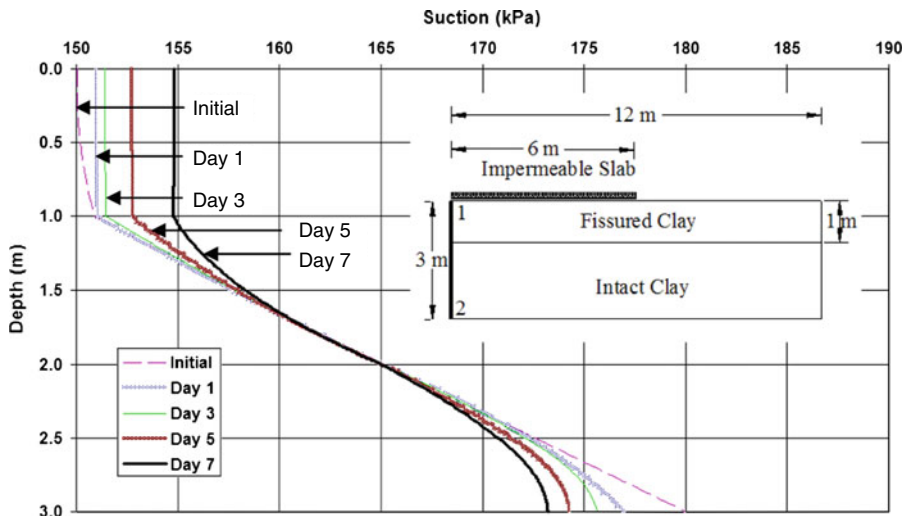

Fig. 19 Changes in matric suction beneath the center o the slab (from point 1 to 2) for evaporation. Crack width of 0.05 mm at a spacing of 10 cm, initial soil suction greater than the Air Entry Value of the cracked soil

(Fig. 25). Horizontal flow dominates in the cracked soil and in the entire cross-section.

The increase of soil suction with depth at the center of the slab and below the edge of the slab occurred rapidly, as shown in Fig. 22 for a vertical profile beneath the center of the slab. This occurs due to the high hydraulic conductivity of the cracked soil. Figures 14 and 21 (both with crack width of 0.05 mm and crack spacing of 0.5 cm), show that when the initial suction value is lower than the air-entry value of the cracked soil there is relatively less horizontal flow and suctions beneath the slab do not change significantly (Fig. 14). However, when the initial suctions are greater than the air-entry value of the cracked soil there is significant horizontal flow and the suctions beneath the slab change significantly as evaporation proceeds both horizontally and with depth (Figs. 21, 22).

A crack depth of 2 m was also evaluated for evaporation for both high and low initial suction conditions. Trends were similar to those observed for the 1 m crack depth except that suctions at the ground surface were greater for the 2 m crack depth than for the 1 m crack depth.

17 Simulation of Infiltration Conditions

The initial conditions for the simulation of water infiltration were obtained from a steady state analysis. The infiltration rate for the transient analyses was

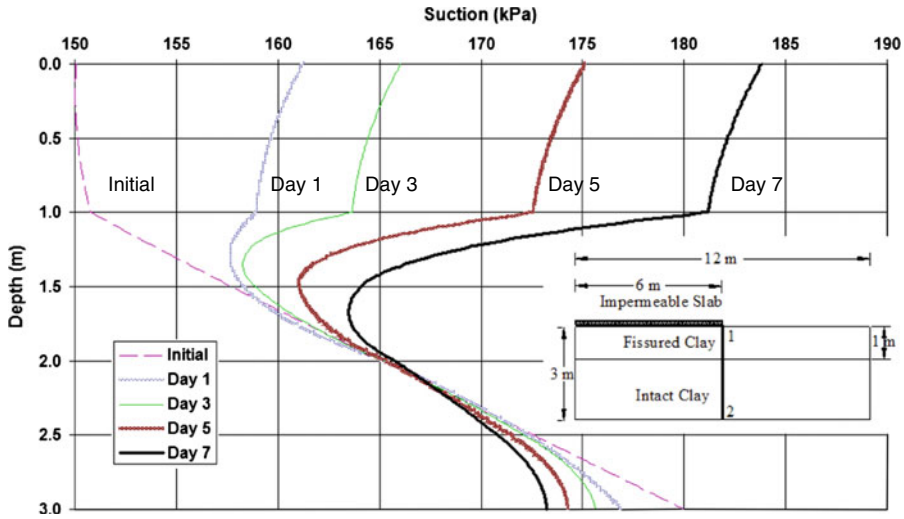

Fig. 20 Changes in matric suction beneath the edge of the slab (from point 1 to 2) for evaporation. Crack width of 0.05 mm at a spacing of 10 cm, initial suction greater than the Air Entry Value of the cracked soil

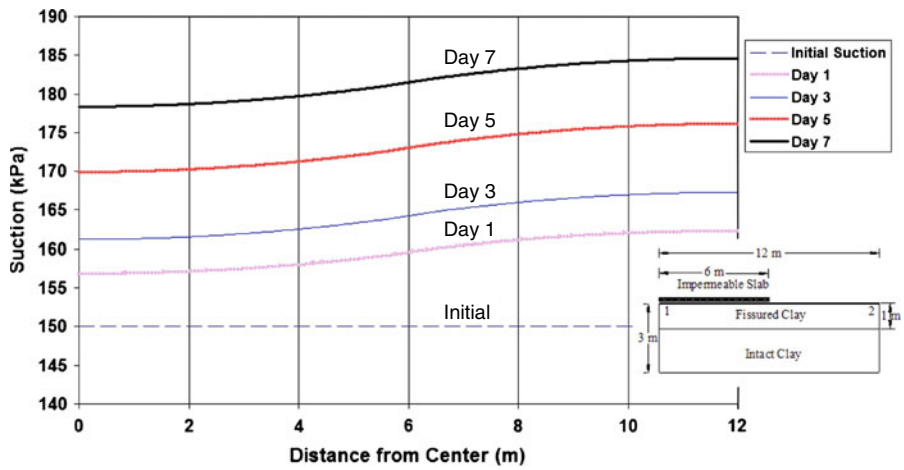

Fig. 21 Changes in matric suction along the ground surface (from point 1 to 2) for evaporation. Crack width of 0.05 mm at a spacing of 0.5 cm, initial suction greater than the Air Entry Value of the cracked soil

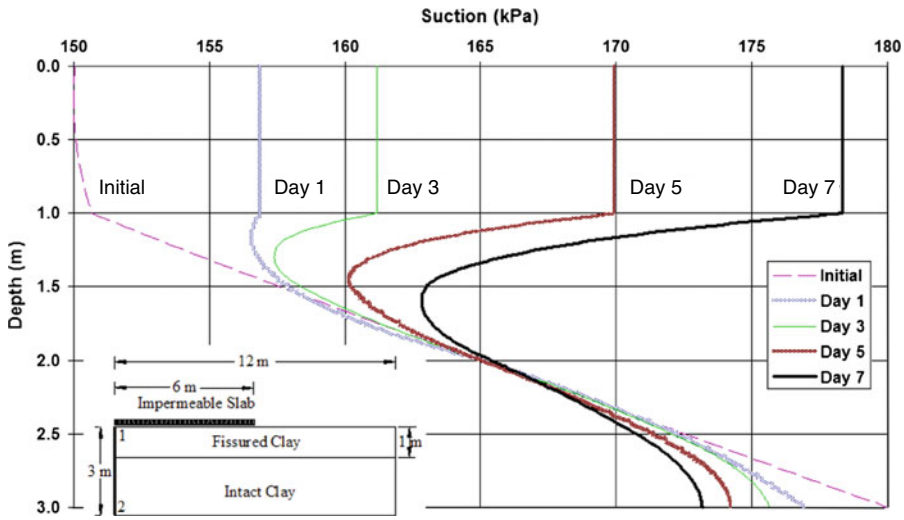

Fig. 22 Changes in matric suction beneath the center of the slab (from point 1 to 2) for evaporation. Crack width of 0.05 mm at a spacing of 0.5 cm,initial suction greater than the Air Entry Value of the cracked soil

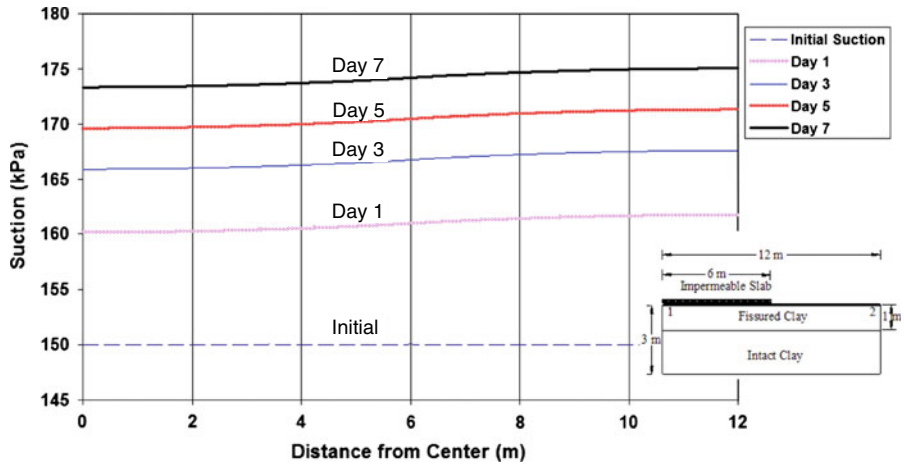

Fig. 23 Changes in matric suction along the ground surface (from point 1 to 2) for evaporation. Crack width of 1 mm at a spacing of 10 cm, initial soil suction greater than the Air Entry Value of the cracked soil

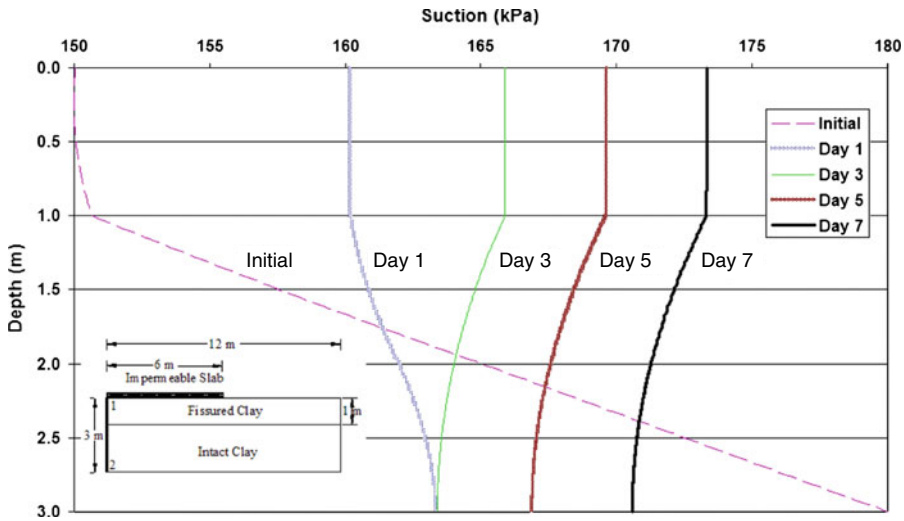

Fig. 24 Changes in matric suction beneath the center of the slab (from point 1 to 2) for evaporation. Crack width of 1 mm at a spacing of 10 cm, initial soil suction greater than the Air Entry Value of the cracked soil

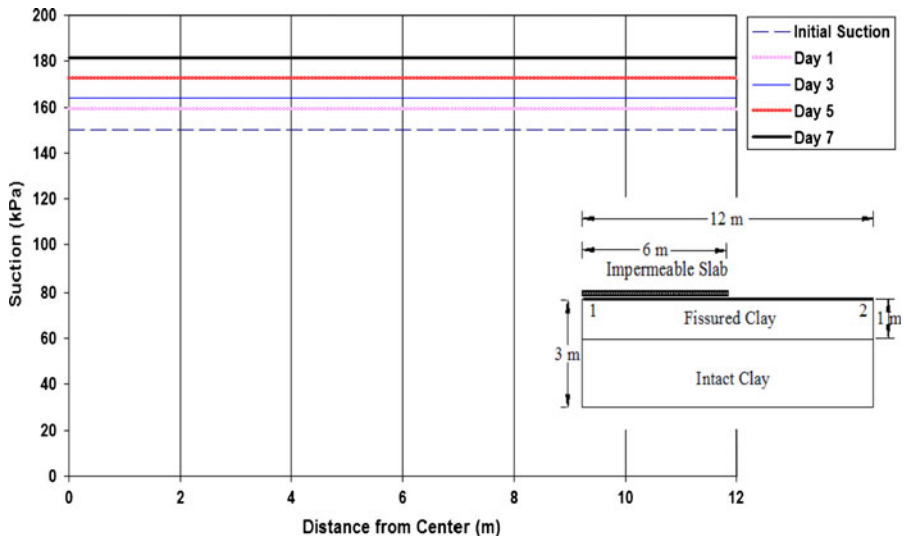

Fig. 25 Changes in matric suction along the ground surface (from point 1 to 2) for evaporation. Crack width of 1 mm at a spacing of 0.05 cm, initial value of suction greater than the Air Entry Value of the cracked soil

chosen as being equal in magnitude to the evaporation rate (i.e., 4 mm/day). In this way a comparison can be made between behavior under infiltration and evaporation conditions. Transient analyses were performed for the case of: 1.) no cracks in the soil, 2.) cracks down to 1 m, and 3.) cracks down to 2 m depths. The boundary conditions are the same as those depicted in Fig. 8, and a surface infiltration of 4 mm/day was applied on the exposed ground surface.

18 Infiltration of Intact Clay: No Cracks and Low Initial Suction

Because the initial matric suction at the ground surface was low and the intact hydraulic conductivity of the clay was low, there was little infiltration into the "initially wet" intact clay over the infiltration period of 7 days considered in this study. Hence, the suction profiles beneath the slab and outside of the slab were essentially identical and essentially the same as for the initial conditions imposed.

19 Infiltration With Initial Suctions Less Than Air-Entry Value of the Cracked Soil

The numerical analysis of infiltration was performed for 7 days. Figures 26 and 27 show the simulation results for a 1 m depth of fissured soil having a crack width of 0.05 mm at a spacing of 10 cm. The simulation results for the cracked soil with a crack width of 1 mm and a spacing of 10 cm are shown in Figs. 28 and 29 for initial suctions at ground surface less than the air-entry value of the cracked soil.

Higher crack volumes result in higher saturated hydraulic conductivities for the cracked soils as compared to the intact soil. As a consequence, moisture flows mainly through the cracked soil. Horizontal flow was substantial for larger crack volumes, as evidenced by the pattern of surface suction shown in Fig. 28. Consequently, suction values are the same outside of and beneath the impermeable slab.

Matric suctions are distributed linearly (vertically) along the depth of the cracked section of the soil profile due to rapid redistribution of matric suctions resulting from high hydraulic conductivity of the "wet" fractured soil. On the other hand, suctions re-distribute nonlinearly along the depth of the intact clay due to the relatively low hydraulic conductivity of the intact clay (e.g., see Fig. 29).

20 Infiltration With Initial Suctions Greater Than Air-Entry Value of the Cracked Soil

The numerical analysis of infiltration was performed for 7 days for comparison with the infiltration simulations when the initial suctions were less than air-entry value of the cracked soil. Sample results are shown in Figs. 30–32. The cracked volumes

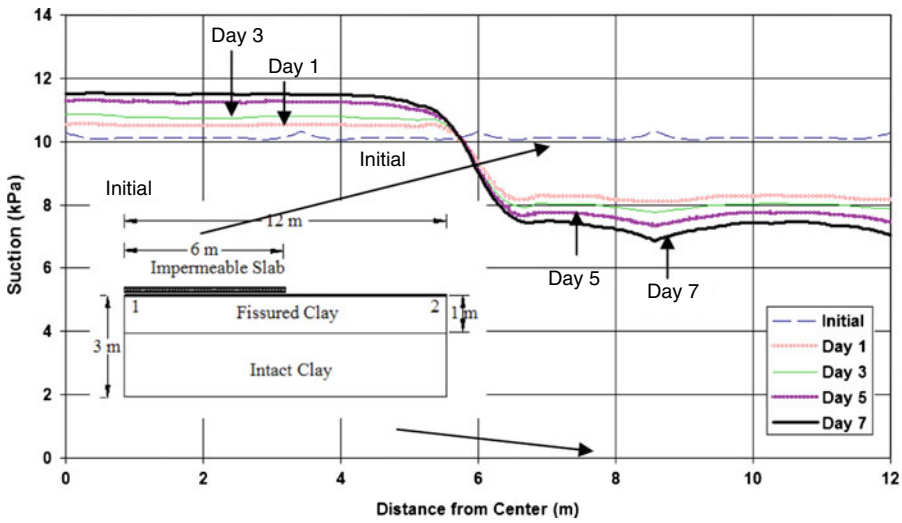

Fig. 26 Changes in matric suctions along the ground surface for infiltration. Crack width of 0.05 mm at a spacing of 10 cm, initial suction less than the Air Entry Value of the cracked soil

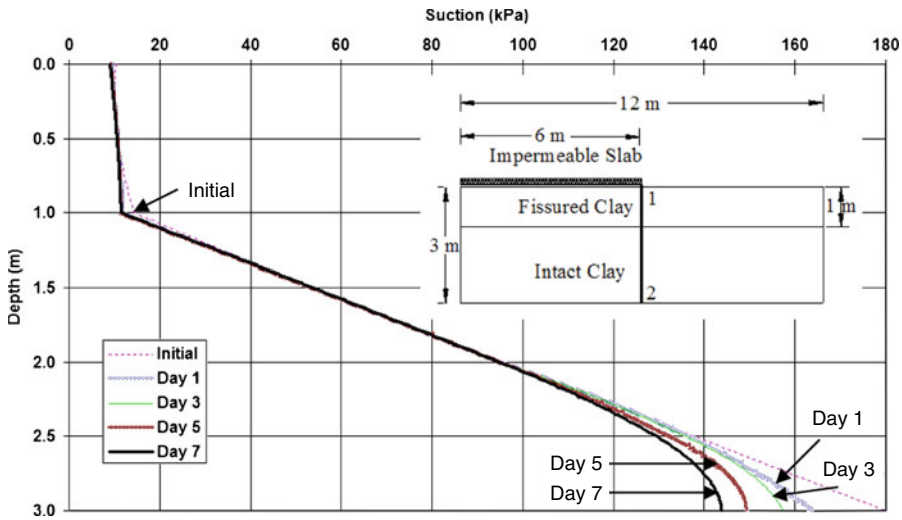

Fig. 27 Changes in matric suction along the edge of the slab (from point 1 to 2) for infiltration. Crack width of 0.05 mm at a spacing of 10 cm, initial suction less than the Air Entry Value of the cracked soil

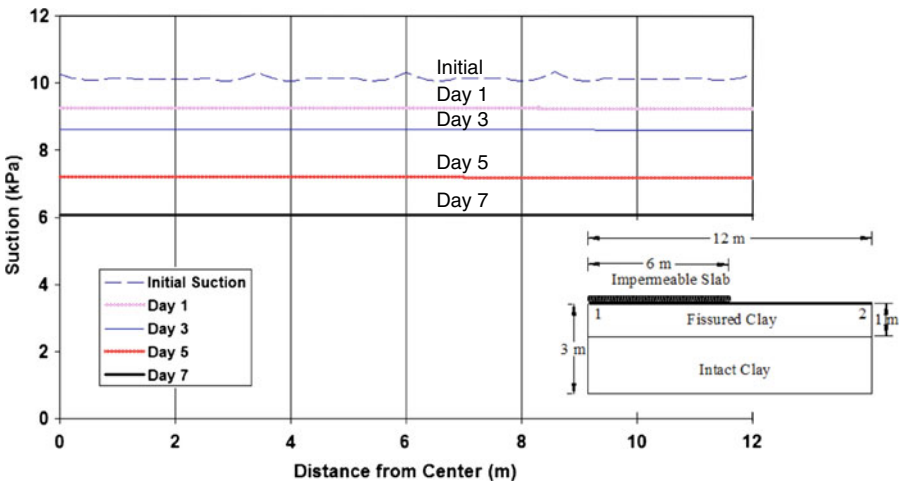

Fig. 28 Matric suction variations along the ground surface (from point 1 to 2) for infiltration. Crack width of 1 mm at a spacing of 10 cm, initial suction less than the Air Entry Value of the cracked soil

considered for the infiltration case with relatively high initial ground surface suctions correspond to a crack width of 0.05 mm at a spacing of 10 cm (i.e., a relatively low crack volume).

The hydraulic conductivity of the cracked soil is relatively low at high suctions (i.e., higher than the air-entry value of the fractured soil), and therefore the changes in matric suction occur mainly under the uncovered area. The horizontal flow is not large and the soil suctions are essentially unchanged under the covered area (Figs. 30, 31). However, the relatively high hydraulic conductivity of the cracked soil (compared to the intact clay), results in near-vertical profiles of suction in the cracked region, (compared to more or less linearly increasing suction with depth for the intact clay portion) (Fig. 32).

A crack depth of 2 m was also evaluated for infiltration, and the results were similar to those for the 1 m deep cracks. Values of surface matric suction were not significantly lower for the 2 m crack depth as compared to the 1 m crack depth.

21 Suction Beneath the Slab as Related to Initial Conditions for Infiltration

Depending on the initial conditions of suctions and the specific distribution of matric suctions with depth

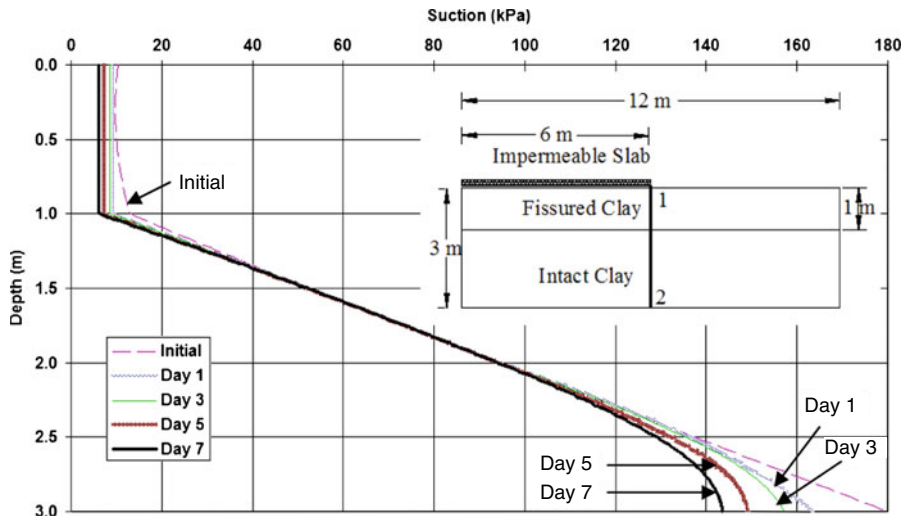

Fig. 29 Changes in matric suction beneath the edge of the slab (from point 1 to 2) for infiltration. Crack width of 1 mm at a spacing of 10 cm, initial suction less than the Air Entry Value of the cracked soil

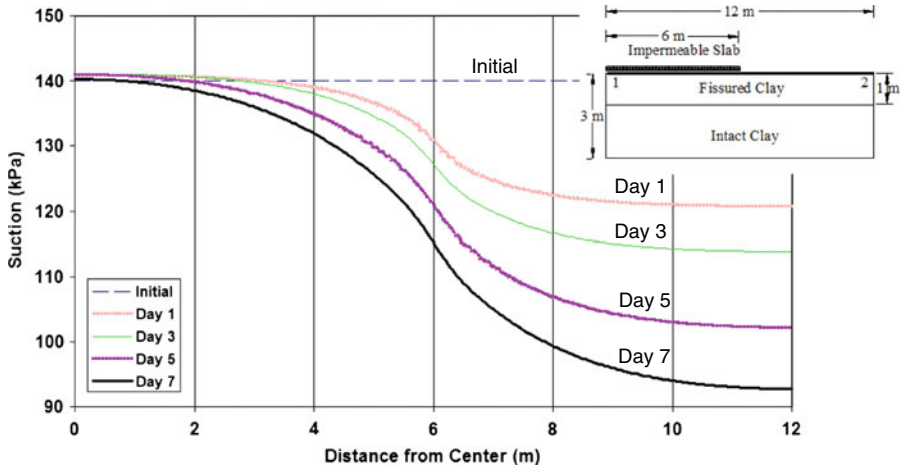

Fig. 30 Matric suctions changes along the ground surface (from point 1 to 2) for infiltration. Crack width of 0.05 mm at a spacing of 10 cm, initial suction greater than the Air Entry Value of the cracked soil

in the soil, and the hydraulic conductivity of the cracked soil, the matric suctions can increase or decrease with time under the slab for infiltration conditions (see Figs. 26, 28, 30). The matric suctions always decrease in the uncovered soil during infiltration. However, soil suctions under the slab may increase when there is a low volume of cracks, depending upon the magnitude and distribution of soil suction at depth. An increase of the matric suctions beneath the covered area during infiltration can be seen in Fig. 26 for the case where the initial soil suction is less than the air-entry value of the cracked soil. The increase in suction beneath the slab is a result of downward moisture flow caused by high initial base boundary soil suction conditions (see initial suction profile in Fig. 27).

22 Discussion and Conclusions

If a soil contains cracks its physical behavior can be assumed to be bi-modal in character. The bi-modal soil behavior will be exhibited in the soil–water characteristic curve which in turn, affects the calculation of water storage as well as the hydraulic conductivity function. In this study, a bimodal model was used to represent a cracked soil. The cracked soil was used to simulate possible moisture movement conditions associated with slab-on-ground foundations on clay soil profiles with cracks near to the ground surface. Several tentative conclusions can be drawn from the simulations of evaporation and infiltration from a cracked soil.

A cracked soil behaves as if it is the combination of two materials. Consequently, the soil–water

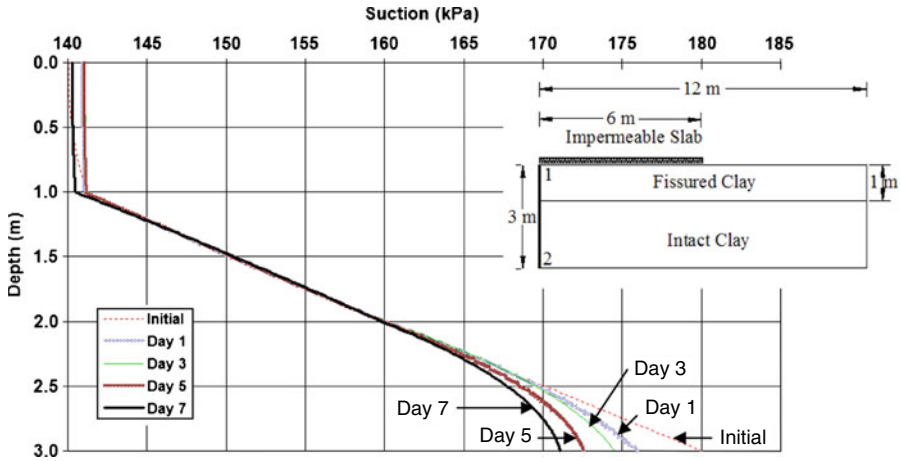

Fig. 31 Changes in matric suction along beneath the center of the slab (from point 1 to 2) for infiltration. Crack width of 0.05 mm at a spacing of 10 cm, initial suction greater than the Air Entry Value of the cracked soil

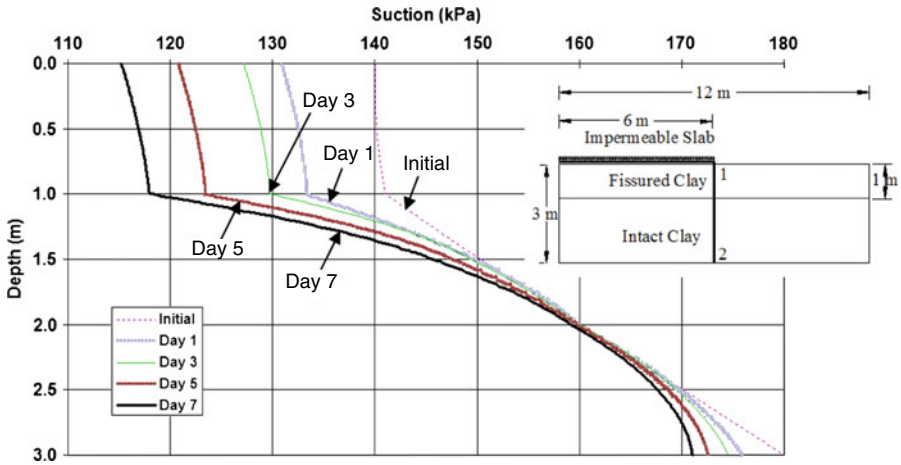

Fig. 32 Changes in matric suction beneath the edge of the slab (from point 1 to 2) for infiltration. Crack width of 0.05 mm at a spacing of 10 cm, initial suction greater than the Air Entry Value of the cracked soil

characteristic curve and the hydraulic conductivity functions can be considered to be bi-modal in character from a continuum mechanics standpoint. The unsaturated soil property functions for the cracked soil (e.g., hydraulic conductivity, water storage), are initially treated as being two independent materials and then the results are combined. The SWCC is obtained for each material starting from saturated conditions. Super-position is used to obtain the soil property function of the overall cracked soil. It is noted that the unsaturated hydraulic conductivity functions for a cracked soil cannot be obtained by simply integrating along the bimodal SWCC.

Cases of infiltration and evaporation at the ground surface were considered for an intact soil which was then compared to the results for a cracked soil. The results show that for intact clay there is a high suction gradient at the edge of the slab at the ground surface but matric suctions are not changing significantly under the covered area for the 7 day flux conditions considered in this study. By contrast, when a significant volume of soil with cracks is present, matric suctions quickly becomes essentially uniform along the ground surface, irrespective of the impermeable slab covering a portion of the soil. This is due to increased hydraulic conductivity of the cracked soil as compared to that of the intact clay. The end result is a dominance of horizontal flow in the cracked soil region.

Essentially vertical (constant with depth) matric suction profiles were observed in the cracked soil regions as a result of evaporation and infiltration at the ground surface but soil suctions in the lower intact portion of the profile varied significantly with depth (nonlinearly and/or linearly). This behavior appears to be due to the higher conductivity and lower gradient

in the cracked soil as compared to the lower conductivity and higher gradients in the intact soil.

The magnitude of soil matric suction change increases with increasing crack volume, both for evaporation and infiltration conditions. When there is a substantial volume of cracks in the soil, the matric suctions are essentially uniform along the ground surface. The same behavior is observed for both the evaporation and infiltration and whether the initial suction is higher or lower than the air-entry value of the cracked soil.

Ground surface matric suctions increase during evaporation and decrease during infiltration in uncovered soil regions. When cracks occur in the soil and suctions along the surface are less than the air-entry value of the cracked soil, the matric suctions can increase or decrease under a covered area during infiltration conditions. This behavior depends on the magnitude and distribution of matric suction with depth. However, for the infiltration case when the initial suctions are greater than the air entry value of the cracked soil, the soil suction beneath the slab decreases. In the case of a low crack volume, the matric suctions remain relatively stable beneath the slab as compared to the region outside the slab. Although not considered in this study, longer periods of infiltration (or evaporation) would result in further wetting (or drying) than that observed for the 7-day simulations performed. However, in the case of a large crack volume, matric suction changed substantially both outside of the slab and beneath the slab for the 7 day simulations.

The above conclusions are based on the inherent assumptions built into the unsaturated soil property functions for the cracked soil, namely that the cracked soil can be treated as a continuum and that the SWCC and hydraulic conductivity functions can be represented as a bi-modal function. Currently data is not available for validation of the modeling results. Nonetheless, the results of this parametric study establish a beginning point for evaluation of the effect of soil cracking on suction variations with a soil profile. Certain aspects of cracked clay behavior such as volume change, anisotropy, and hysteresis, have not been incorporated into the continuum model of this study, and further studies are needed to evaluate the impact of these cracked soil behavior characteristics on unsaturated flow, suction variation, and soil deformation.

Acknowledgments This work was supported by the Homebuilders' Association of Central Arizona, and in part by NSF under grant no. CMMI-0825089. The views presented in this paper are those of the authors and not necessarily those of the Homebuilders' Association of Central Arizona.

References

Assouline S (2001) A model for soil relative hydraulic conductivity based on the water retention characteristic curve. Water Resour Res 37:265–271

Barenblatt GI, Zheltov IP, Kochina IN (1960) Basic concepts in the theory of seepage of homogeneous liquids in fissured rocks. J Appl Math 24:1286–1303

Berkowitz B (2002) Characterizing flow and transport in fractured geological media: a review. Adv Water Resour 25:861–884

Brooks RH, Corey AT (1964) Hydraulic properties of porous media. Colorado State University Hydrology Paper, Fort Collins, Nr. 3, vol. 27, March

Burdine NT (1953) Relative permeability calculation size distribution data. Transactions of the American Institute of Mining. Metallur Petrol Eng 198:71–78

Burger CA, Shackelford CD (2001) Soil-water characteristic curves and dual porosity of sand-diatomaceous earth mixtures. J Geotech Geoenviron Eng ASCE 127(9):790–800

Campbell JD (1973) Pore pressures and volume changes in unsaturated soils. Ph.D. thesis, University of Illinois at Urbana, Champaign, Urbana-Champaign, IL, USA

Carman PC (1939) Permeability of saturated sands, soils and clays. J Agric Sci 29:262–273

Chertkov VY, Ravina I (2000) Shrinking-swelling phenomenon of clay soils attributed to capillary-crack network. Theor Appl Fract Mech 34:61–71

Durner W (1994) Hydraulic conductivity estimation for soil with heterogeneous pore structure. Water Resour Res 30(2):211–223

Fredlund MD (1996) SoilVision users guide, Version 2.0, Edition 1.0. SoilVision Systems Ltd, Saskatoon

Fredlund DG, Rahardjo H (1993) Soil mechanics for unsaturated soils. Wiley, New York

Fredlund DG, Xing A (1994) Equations for the soil-water characteristic curve. Can Geotech J 31:521–532

Gardner WR (1958) Some steady-state solutions of unsaturated moisture flow equations with application to evaporation from a water table. Soil Sci 85:228–232

Gitirana G Jr, Fredlund DG (2004) Equations for the soil-water characteristic curve based on meaningful and mathematically independent parameters, technical note. ASCE J Geotech Environ Eng 130(2):209–212

Irmay S (1954) On the hydraulic conductivity of unsaturated soils. Transactions of the American Geophysical Union, vol 35

Irmay S (1971) A model of flow of liquid-gas mixtures in porous media and hysteresis of capillary potential. Israel Institute of Technology, Haifa

Kazemi H (1969) Pressure transient analysis of naturally fractured reservoirs with uniform fracture distribution. Soc Petrol Eng J 451–62. Trans AIME 246

Kazemi H (1979) Numerical simulation of water imbibition in fractured cores. Soc Petrol Eng J 323–330

Keller CK, van der Kamp G, Cherry JA (1985) Fracture permeability and groundwater flow in clayey till near Saskatoon, Saskatchewan. Can Geotech J 23:229–240

Köhne JM, Köhne S, Gerke HH (2002) Estimating the hydraulic functions of dual-permeability models from bulk soil data. Water Resour Res 38(7):1121–1132

Kozeny J (1927) Ueber Kapillare Leitung des Wassers im Boden. Wien AkadWiss 136(2a):271

Kunze RJ, Uehara G, Graham K (1968) Factors important in the calculation of hydraulic conductivity. Soil Sci Soc Am Proc 32:760–765

Leong EC, Rahardjo H (1997) Review of soil-water characteristic curve equations. J Geotech Eng Div ASCE 123(12):1106–1117

Liu HH, Bodvarsson GS (2001) Constitutive relations for unsaturated flow in a fracture network. J Hydrol 252: 16–25

Liu HH, Bodvarsson GS, Finsterle S (2004) A note on unsaturated flow in two-dimensional fracture networks. Technical note. Earth Sciences Division. Lawrence Berkeley National Laboratory. University of California, Berkeley California

Mallant D, Tseng PH, Torde N, Timmerman A, Feyen J (1997) Evaluation of multimodal hydraulic function in charactering a heterogeneous field soil. J Hydrol 195:172–199

Mualem Y (1976) A new model for predicting the hydraulic conductivity of unsaturated porous media. Water Resour Res 12:593–622

Novák V, Simunek J, van Genuchten MTh (2000) Infiltration into soil with fractures. J Irrig Drain Eng 126(1):41–47

Odeh AS (1965) Unsteady-state behavior of naturally fractured reservoirs. J Soc Petrol Eng 3:60–64

Peters RR, Klavetter EA (1988) A continuum model for water movement in unsaturated fractured rock mass. Water Resour Res 24(3):416–430

Pruess K, Narasimhan TN (1985) A practical method for modeling fluid and heat flow in fractured porous media. Soc Petrol Eng J 25:14–26

Sillers WS, Fredlund DG, Zakerzadeh N (2002) Mathematical attributes of some soil-water characteristics curve models. Geotech Geol Eng J 19:243–283

Snow DT (1965) A parallel plate model of fractured permeable media, Ph.D. dissertation, University of California, Berkeley, 331 p

Stothoff S, Or D (2000) A discrete-fracture boundary integral approach to simulating coupled energy and moisture transport in a fractured porous medium. In: Faybishenko B, Witherspoon PA, Benson SM (eds) Dynamics of fluids in fractured rocks, concepts, and recet advances. AGU Geophysical Monograph 122

van Genuchten M Th (1980) A closed form equation for predicting the hydraulic conductivity of unsaturated soils. Soil Sci Soc Am J 44:892–898

Warren JE, Root PJ (1963) The behavivor of naturally fractured reservoirs. Soc Petrol Eng J 245–255. Trans AIME 228

Wu TH (1976) Soil mechanics, 2nd edn. Allyn asnd Bacon, Boston

Wu YS (2000) On the effective continuum method for modeling multiphase flow, multi-component transport and heat transfer in fractured rock. In: Faybishenko B, Witherspoon PA, Benson SM (eds) Dynamics of fluids in fractured rocks, concepts, and recent advances. AGU Geophysical Monograph 122

Wu YS, Pruess K (2005) A physically based numerical approach for modeling fracture-matrix interaction in fractured reservoirs. In; Proceedings world geothermal congress 2005, Antalya, Turkey, 24–29 April 2005, pp 1–8

Wu YS, Haukwa C, Bodvarsson GS (1999) A site-scale mmodel for fluid and heat flow in the unsaturated zone of Yucca Mountain, Nevada. J Contam Hydrol 38(1–3): 185–217

Zhang L, Fredlund DG (2004) Characteristics of water characteristic curves for unsaturated fractured rocks. In: The second Asian conference on unsaturated soils, Unsat-Asia, Osaka, Japan, pp 425–428